JACS Au
AN OPEN ACCESS JOURNAL OF THE AMERICAN CHEMICAL SOCIETY

pubs.acs.org/jacsau
Article

Monophosphoryl Lipid A–2,4-Dinitrophenylamine Conjugates Are Potent Adjuvants for Carbohydrate and Protein Vaccines

Jiatong Guo,[§] Rajendra Rohokale,[§] Sayan Kundu, and Zhongwu Guo*

Cite This: JACS Au 2025, 5, 2210–2222
Read Online

ACCESS | Metrics & More | Article Recommendations | Supporting Information

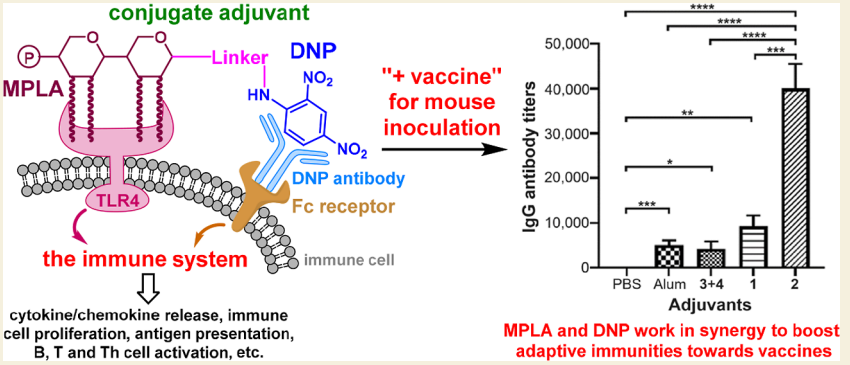

ABSTRACT: Adjuvants are essential for effective vaccine formulation, but currently only a few adjuvants with limited efficacies and application scopes are available. To address this issue, we explored covalent conjugates of monophosphoryl lipid A (MPLA) and 2,4-dinitrophenylamine (DNPA) as a new type of adjuvant. Immunological studies in mice prove that MPLA–DNPA conjugates can help a model vaccine induce robust IgG antibody and adaptive immune responses against carbohydrate and protein antigens and are much more potent adjuvants than alum—the positive control—and the MPLA + DNPA mixture. Detailed profiling and comparison of the cytokines/chemokines elicited by various adjuvants suggest that the MPLA–DNPA conjugates can activate macrophages, monocytes, dendritic, T, T helper, and other immune cells to promote cellular immunity against vaccines. The results suggest a synergistic effect of covalently linked MPLA and DNPA, which act via interacting with the Toll-like receptor and recruiting endogenous anti-DNPA antibodies, respectively. Moreover, the linker between MPLA and DNPA shows a major impact on this synergistic effect, especially for the carbohydrate antigen. Eventually, the MPLA–DNPA conjugate with a longer linker containing a triazole moiety is identified as a promising adjuvant for both carbohydrate and protein vaccines worthy of further research and development.

KEYWORDS: *lipid A, 2,4-dinitrophenyl, glycoconjugates, adjuvants, vaccines*

INTRODUCTION

Vaccines have been employed to successfully control and prevent many infectious diseases and actively pursued for cancer immunotherapy.[1−5] To accomplish effective vaccination, vaccines must be formulated with an adjuvant—the medicines used to enhance immune responses against and efficacies of vaccines.[6−8] Adjuvants can also be used alone to achieve certain therapeutic benefits via generally boosting the immune system.[9−13] Despite their medical significance, presently, only a few adjuvants, such as alum, AS04, MF59, and virosomes, are available for clinical uses in humans.[14−16] Furthermore, these adjuvants have limited efficacies and application scopes. For example, recently approved AS04 and MF59 adjuvants have been applied to formulate only a small number of vaccines,[17] while the broadly adopted adjuvant alum is over a hundred years old and does not exhibit sufficient potencies for many modern vaccines in development. Another problem with current adjuvants is that they are complex mixtures, which hinders their detailed structure–activity relationship (SAR) analysis as well as further improvement and optimization.[6−8]

For the development of antibacterial and antitumor vaccines, special carbohydrates present on bacterial and cancer cells are excellent target antigens due to their unique location on the cell surface to facilitate recognition by and interaction with the immune system. However, carbohydrate antigens are usually poorly immunogenic.[18,19] One of the common strategies to address this issue and improve the efficacies of carbohydrate

Received: February 17, 2025
Revised: April 23, 2025
Accepted: April 24, 2025
Published: April 29, 2025

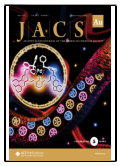

https://doi.org/10.1021/jacsau.5c00187
JACS Au 2025, 5, 2210–2222

vaccines is to combine them with a potent adjuvant.[10,11,20,21] It has been revealed that selecting the appropriate adjuvant to formulate carbohydrate vaccines is vital for successful immunization[22] because each adjuvant has a unique application scope and is suitable for specific vaccines. Unfortunately, current adjuvants are oftentimes not effective for carbohydrate vaccines, especially for carbohydrate-based cancer vaccines. For example, the keyhole limpet hemocyanin (KLH) conjugate of globo H, a tumor-associated carbohydrate antigen (TACA), as a cancer vaccine cannot elicit robust immunities in cancer patients when the conjugate is formulated with traditional adjuvants but becomes functional when it is formulated with QS-21, an experimental saponin adjuvant.[22]

Thus, robust adjuvants with wide application scopes are highly desired for various medical applications.[21] To meet this demand, we synthesized and explored the covalently linked conjugates of monophosphoryl lipid A (MPLA) and 2,4-dinitrophenylamine (DNPA) as a new type of adjuvants, called conjugate adjuvants.[23] Our immunological studies of the MPLA−DNPA conjugates show that they can harness the potent immunostimulatory activities of both MPLA and the 2,4-dinitrophenyl (DNP) motif that possess different action mechanisms. Moreover, these conjugate adjuvants exhibited a synergistic effect. As a result, the MPLA−DNPA conjugates have been demonstrated as potent adjuvants to boost robust and T cell-dependent immunities toward both protein and carbohydrate antigens.

EXPERIMENTAL SECTION

General Methods

Commercial chemicals or materials are used as received without further purification unless noted otherwise. Molecular sieves 4 Å (MS 4 Å) are flame-dried in vacuo and utilized immediately after being cooled to room temperature (rt) under N_2. Analytical TLC is carried out on a silica gel 60 Å F254 plate detected with a UV detector or by charring using 10% (v/v) H_2SO_4 in ethanol. Flash column chromatography is performed with Silica Gel 60 (230−400 mesh). NMR spectra are acquired using a 400 or 600 MHz spectrometer with chemical shifts (δ) reported in reference to $CDCl_3$ (^{1}H: δ 7.26 ppm; ^{13}C: δ 77.16 ppm) or CD_3OD (^{1}H: δ 3.31 ppm; ^{13}C: δ 49.0 ppm). Peaks and coupling constants are assigned on the basis of ^{1}H NMR, ^{1}H−^{1}H COSY, ^{1}H−^{13}C HSQC, and ^{1}H−^{13}C HMBC experiments. MS data are acquired with electrospray ionization (ESI) in the positive or negative mode. alum, DSPC, and cholesterol are purchased from Sigma-Aldrich. AP-linked goat antimouse secondary kappa, IgM, and IgG Abs are purchased from Southern Biotechnology. DNP−OVAL is purchased from Biosearch Technologies. sTn−KLH and sTn−HSA conjugates are synthesized as reported previously. Female C57BL/6 mice of 6−8 weeks of age employed for immunological studies are purchased from The Jackson Laboratory. Upon arrival at the animal facility at the University of Florida (UF), they are examined and kept in cages for 1−2 days to settle in before the experiments start. Animal use protocol for this research (202300000027) is approved by the IACUC of UF.

3-(2,4-Dinitrophenylamino)propanoic Acid (4)

To a solution of β-alanine **5** (0.48 g, 5.37 mmol) and 1-fluoro-2,4-dinitrobenzene **6** (1.0 g, 5.37 mmol) in ethanol (26.0 mL) was added triethylamine (1.5 mL, 10.8 mmol). The solution was heated at 100 °C in the dark for 6 h, cooled to room temperature, and then concentrated in vacuo. The residue was suspended in water, and 2 N HCl was added to pH 1−2. The mixture was extracted with ethyl acetate (3 × 25 mL), and the organic layer was dried with Na_2SO_4 and then condensed. The product was purified on a silica gel column using CH_2Cl_2 and MeOH as eluents to afford **4** (668 mg, 49%) as a yellow solid. TLC: R_f = 0.1 (ethyl acetate/hexane = 4:1). ^{1}H NMR (400 MHz, $CD_3OD/CDCl_3$ = 2:1): δ 9.04 (d, J = 2.7 Hz, 1H), 8.28 (dd, J = 9.6, 2.7 Hz, 1H), 7.12 (d, J = 9.6 Hz, 1H), 4.74 (br, 1H, −N*H*), 3.75 (t, J = 6.5 Hz, 2H, −NHC*H*$_2$−), 2.73 (t, J = 6.5 Hz, 2H, −C*H*$_2$−CO). ^{13}C NMR (101 MHz, $CH_3OD/CDCl_3$ = 2:1): δ 174.2, 149.0, 136.6, 131.2, 130.9, 124.7, 114.9, 39.5, 33.7. HR-ESI-QTOF-MS m/z: calcd for $C_9H_9N_3O_6Na$ $[M + Na]^+$, 255.0491; found, 255.0492.

2,5-Dioxopyrrolidin-1-yl 3-(2,4-Dinitrophenylamino)propanoate (8)

To a solution of **4** (100 mg, 0.39 mmol) in CH_2Cl_2 were added EDC (97.7 mg, 0.51 mmol) and DMAP (9.50 mg, 0.08 mmol) at 0 °C, which was followed by NHS (54.1 mg, 0.47 mmol) 15 min later. The mixture was stirred at rt overnight. After the reaction was completed, as indicated by TLC, the mixture was diluted with CH_2Cl_2. The organic layer was washed with cold saturated $NaHCO_3$ aq solution, water, and brine, dried over Na_2SO_4, and then concentrated in vacuo. The product was purified on a silica gel column to give compound **8** (98.2 mg, 71%) as a yellow solid. TLC: R_f = 0.55 (ethyl acetate/hexane = 4:1). ^{1}H NMR (600 MHz, DMSO-d_6): δ 8.89 (t, J = 8.4 Hz, 1H), 8.87 (d, J = 3.8 Hz, 1H), 8.27 (d, J = 9.4 Hz, 1H), 7.37 (d, J = 9.5 Hz, 1H), 3.87 (t, 2H), 3.16 (t, J = 6.1 Hz, 2H), 2.81 (br, 4H). ^{13}C NMR (151 MHz, DMSO-d_6): δ 170.5, 167.9, 148.4, 135.6, 130.6, 130.5, 124.0, 115.9, 38.7, 30.5, 25.9. HR-ESI-QTOF-MS m/z: calcd for $C_{13}H_{12}N_4O_8Na$ $[M + Na]^+$, 352.0655; found, 352.0658.

3-(2,4-Dinitrophenylamino)-*N*-(prop-2-yn-1-yl)-propenamide (9)

To a solution of **4** (210 mg, 0.82 mmol) in CH_2Cl_2 were added EDC (316 mg, 1.65 mmol) and DMAP (10.0 mg, 0.08 mmol) at 0 °C. About 15 min later, propargyl amine (68.0 mg, 1.23 mmol) was added, and the mixture was stirred at rt overnight. After adding CH_2Cl_2, the organic layer was washed with saturated $NaHCO_3$ aq solution, water, and brine and dried over Na_2SO_4. The solution was concentrated in vacuo, and the residue was purified by silica gel column chromatography to provide compound **9** (209 mg, 87%) as a yellow solid. TLC: R_f = 0.6 (ethyl acetate). ^{1}H NMR (600 MHz, CD_3OD): δ 9.03 (d, J = 2.4 Hz, 1H), 8.30 (dd, J = 9.6, 2.8 Hz, 1H), 7.21 (d, J = 9.6 Hz, 1H), 3.96 (d, J = 2.1 Hz, 2H, −NH−C*H*$_2$−CC), 3.78 (t, J = 6.5 Hz, 2H, −NH−C*H*$_2$−), 2.63 (t, J = 6.5 Hz, 2H, −C*H*$_2$−CO), 2.56 (td, J = 2.6, 0.8 Hz, 1H, acetylene). ^{13}C NMR (151 MHz, CH_3OD): δ 172.8, 149.5, 137.1, 131.1, 124.8, 115.6, 80.4, 72.3, 40.52, 35.5, 29.5. HR-ESI-QTOF-MS m/z: calcd for $C_{12}H_{12}N_4O_5Na$ $[M + Na]^+$, 292.0808; found, 298.0810.

MPLA−DNP Conjugate 1

To a solution of **3** (9.20 mg, 5.48 μmol) in CH_2Cl_2 (3.0 mL) and DMF (1.0 mL) were added NHS-activated ester **8** (3.86 mg, 11.0 μmol) and *N*-methylmorpholine (6.0 μL, 54.9 μmol) at 0 °C. The mixture was stirred at rt for 2 d when the reaction was completed, as indicated by TLC. The mixture was concentrated, and the residue was purified on a silica gel column and then on an LH-20 column with $CHCl_3$ and CH_3OH (3:1) as the eluents to afford **1** (7.34 mg, 54%) as a yellowish glassy solid. TLC: R_f = 0.4 ($CHCl_3$/MeOH = 4:1). ^{1}H NMR (600 MHz, $CDCl_3/CD_3OD/D_2O$ = 2:1:0.2): δ 9.07 (d, J = 2.3 Hz, 1H, ArH), 8.27 (dt, J = 9.7, 2.7 Hz, 1H, ArH), 7.28 (d, J = 6.8 Hz, 1H), 7.24 (d, J = 8.7 Hz, 1H, −CON*H*), 7.22 (d, J = 7.2 Hz, 1H, −CON*H*), 7.12 (d, J = 9.9 Hz, 1H, ArH), 5.23−5.01 (m, 4H), 4.91 (t, J = 8.1 Hz, 1H), 4.58−4.45 (m, 2H, 1H-anomeric), 4.31 (d, J = 9.0 Hz, 1H, anomeric), 4.26−4.15 (m, 2H), 4.14 (dd, J = 5.1, 3.3 Hz, 1H), 4.08−3.82 (m, 10H), 3.80−3.65 (m, 6H), 3.65−3.60 (m, 1H), 3.57 (dd, J = 6.8, 2.4 Hz, 1H), 3.54−3.48 (m, 1H), 3.47−3.38 (m, 2H), 2.72−2.60 (m, 2H), 2.52−2.18 (m, 14H), 1.61−1.43 (m, 11H), 1.30−1.19 (m, 105H), 0.84 (t, J = 7.1 Hz, 18H). ^{13}C NMR (151 MHz, CH_3OD): δ 174.4, 174.3, 173.0, 172.9, 172.0, 171.9, 171.7, 148.7, 136.2, 130.7, 128.9, 124.6, 114.9, 102.0, 101.4, 76.4, 76.2, 75.3, 75.0, 74.9, 74.4, 71.5, 69.1, 68.8, 68.3, 68.2, 65.2, 63.7, 54.4, 50.9, 43.0, 42.7, 42.6, 42.3, 41.5, 41.4, 40.1, 40.0, 37.9, 37.7, 37.6, 37.4, 37.3, 34.9, 34.5, 34.4, 34.3, 34.3, 32.3, 32.0, 31.9, 30.4, 30.0, 29.7, 29.6, 26.0, 26.0, 25.9, 25.6, 25.4, 23.0, 14.3. ^{31}P NMR (243 MHz,

https://doi.org/10.1021/jacsau.5c00187
JACS Au 2025, 5, 2210−2222

CH_3OD): δ −2.62. HR-ESI-QTOF-MS m/z: calcd for $C_{99}H_{185}N_8O_{27}P$ $[M + NH_4]^+$, 1931.2738; found, 1931.2766.

MPLA−DNP Conjugate 2

To a solution of **3** (17.0 mg, 7.58 μmol) in CH_2Cl_2 (3.0 mL) and MeOH (1.0 mL) was added imidazole-1-sulfonyl azide hydrochloride **10** (3.17 mg, 15.1 μmol) at 0 °C, which was followed by the addition of sodium acetate (1.55 mg, 18.9 μmol) and $CuSO_4{\cdot}5H_2O$ (0.18 mg, 0.01 μmol) in MeOH (0.5 mL). The mixture was stirred at rt for 1 day and filtered through a Celite pad. The solvents were removed in vacuo. The crude product **11** (∼12 mg) was then dissolved in a 1:1 mixture of MeOH and CH_2Cl_2 (2.0 mL), and alkyne **9** (8.24 mg, 28.18 μmol) was added, followed by sodium ascorbate (1.51 mg, 7.05 μmol) and $CuSO_4{\cdot}5H_2O$ (0.35 μg, 1.41 μmol) in MeOH (0.5 mL). The reaction mixture was stirred at rt for 1 d. After the reaction was completed, the mixture was filtered through a Celite pad, and the solvents were removed in vacuo. The product was purified on a silica gel column and then on an LH-20 column with $CHCl_3$ and CH_3OH (3:2) as the eluent to afford **2** (5.74 mg, 41%) as a yellowish glassy solid. TLC: R_f = 0.3 ($CHCl_3$/MeOH = 9:1). ^{1}H NMR (600 MHz, $CDCl_3/CD_3OD/D_2O$ = 2:1:0.2): δ 9.06 (d, J = 2.6 Hz, 1H), 8.23 (dd, J = 9.6, 2.9 Hz, 1H), 7.73 (br, 1H, triazole-*H*), 7.07 (dd, J = 9.6, 3.4 Hz, 1H), 5.17−4.97 (m, 4H), 4.88 (t, J = 9.3 Hz, 1H), 4.56−4.44 (m, 3H, 1H-anomeric), 4.43−4.37 (m, 1H), 4.36 (d, J = 8.3 Hz, 1H, anomeric), 4.24−4.12 (m, 2H), 3.98−3.7 (m, 6H), 3.78−3.60 (m, 6H), 3.50 (dd, J = 7.3, 6.0 Hz, 1H), 3.45−3.39 (m, 1H), 2.74−2.63 (m, 2H), 2.50−2.14 (m, 12H), 1.21 (s, 124H), 0.83 (t, J = 7.1 Hz, 18H). ^{13}C NMR (151 MHz, CH_3OD): δ 130.6, 124.5, 124.4, 114.6, 101.7, 101.3, 75.9, 75.4, 75.1, 74.3, 71.7, 71.4, 70.5, 69.1, 69.0, 68.8, 68.6, 68.5, 67.8, 56.2, 54.1, 53.8, 50.7, 45.9, 45.7, 42.4, 42.1, 41.4, 39.9, 39.1, 37.7, 37.6, 37.5, 37.5, 35.1, 35.0, 34.8, 34.8, 34.5, 34.3, 33.0, 32.2, 30.2, 29.8, 27.8, 25.9, 25.6, 25.3, 24.1, 23.0, 14.2. ^{31}P NMR (243 MHz, CH_3OD): δ −2.70. HR-ESI-QTOF-MS m/z: calcd for $C_{102}H_{182}N_9O_{27}P$ $[M + 2H]^{2+}$, 998.1436; found, 998.1454.

HPLC Analysis of the Conjugate Adjuvants 1 and 2

HPLC was carried out with a Waters e2695 Alliance HPLC system using a 2424 ELSD detector running MassLynx 4.1 software. Chromatography was performed with a Hypersil GOLDTM-C8 column (150 × 4.6 mm; particle size: 5 μ) at 30 °C. The ELSD conditions were optimized as a drift tube temperature of 25 °C and nitrogen gas pressure of 4 bar. The injection volume was 3.0 μL. The mobile phase consisted of methanol and water (40:60, v/v) containing 0.01 mM ammonium formate, running in an isocratic mode with a 1 mL/min flow rate. The HPLC retention time of **1** and **2** was 5.41 and 6.24 min, and purity was >97% and >91%, respectively.

General Procedure for the Preparation of Liposomes of Adjuvants

The mixture of MPLA−DNP conjugate **1** or **2** (0.48 μmol) or of (**3** + **4**) mixture (1:1, 0.48 μmol total), DSPC (2.45 mg, 3.10 μmol), and cholesterol (0.92 mg, 2.38 μmol) (10:65:50 molar ratio) was dissolved in a mixture of CH_2Cl_2 and MeOH (1:1, v/v, 2 mL) in a 10 mL round-bottomed flask. The solvents were removed in vacuo with a rotary evaporator to generate a thin lipid film on the flask wall, which was followed by adding HEPES buffer (20 mM, pH 7.5, 2.0 mL) containing NaCl (150 mM) for lipid hydration. The mixture was shaken under argon at 40 °C for 1 h, and the resultant milky suspension was sonicated for 1 min to obtain the desired liposomes, which were preserved at 4 °C before usage as the adjuvant for immunizations. Each of these liposome suspensions (20 μL) was also diluted with phosphate-buffered saline (PBS) buffer to a final volume of 500 μL to perform dynamic light scattering (DLS) analysis using a Malvern DLS instrument.

Immunization of Mice

Each group of six female C57BL/6 mice of 6−8 weeks of age was first inoculated 4 times (once per week) with a preparation (0.1 mL) of DNP−OVAL (containing 8.0 μg of DNP) and alum via s.c. injection. Blood samples were collected before inoculation (D_{-28}, i.e., 28 days before vaccination with sTn−KLH) and a week after the fourth inoculation (D_0, i.e., a day before vaccination with sTn−KLH) to analyze anti-DNP Abs. Thereafter, mice were vaccinated with an sTn−KLH preparation (0.1 mL total volume containing 8.0 μg of sTn per injection) formulated in 50 μL of PBS plus 50 μL of PBS, alum, or the liposomal solution of adjuvant **1**, **2**, or **3** + **4** via s.c. injection using a 26G 1/2 (0.45 mm 13 mm) needle on days 1, 15, 22, and 29, respectively. Blood samples were collected from each mouse by the saphenous vein on days 0 (prior to the initial immunization) and days 28 and 36 (a week after the third and fourth immunizations). The mouse inoculation and blooding schedules are outlined in Figure 2A. Mouse sera were prepared from collected blood samples by conventional protocols and stored at −80 °C before further investigation.

ELISA Protocols

To examine anti-DNP Abs in the mouse sera, 96-well plates were coated with the DNP−BSA conjugate (2.0 μg/mL, 100 μL/well) in a coating buffer (0.1 M bicarbonate, pH 9.6) at 4 °C overnight. The plates were incubated at 37 °C for 1 h and washed 3 times with washing buffer PBST (PBS containing 0.05% Tween-20). Then, the plates were blocked with blocking buffer (1% BSA in PBST, 200 μL/well) at rt for 2 h. After being washed 3 times, pooled D_{-28}, D_0, and D_{36} mouse sera in a 1:50 dilution using PBS were added to the plates (100 μL/well), followed by 2 h of incubation at 37 °C. The plates were washed 3 times, and antimouse kappa, IgG, or IgM Abs were added to the plates at a dilution of 1:1000 in PBS (100 μL/well), followed by incubation at rt for 1 h. The plates were washed 3 times, and *p*-nitrophenyl phosphate (PNPP) dissolved in a buffer (1.67 mg/mL) was added (100 μL/well). After 30 min of incubation, the light absorbance at 405 nm wavelength was measured using a BioTek plate reader. For the Ab titer analysis, the resultant optical density (OD) values were plotted against antiserum dilution values to obtain a best-fit line. The equation of this line was used to calculate the dilution value at which an OD value of 0.1 was achieved, while the Ab titer was the inverse of this dilution value.

To specifically detect anti-sTn and anti-KLH Abs, a solution of sTn−HSA conjugate or KLH protein (2.0 μg/mL, 100 μL) in the coating buffer (0.1 M bicarbonate, pH 9.6) was respectively added to the wells of ELISA plates, and the plates were incubated at 37 °C for 1 h, followed by washing with PBST 3 times. The blocking solution (100 μL/well) was added, and after incubation at 37 °C for 1 h, the plates were washed with PBST 3 times. Then, a pooled day 1 serum or an individual antiserum with serial half-log dilution from 300 to 218,700 in PBS was added to the plate (100 μL/well), which was followed by incubation at 37 °C for 2 h. The plates were washed with PBS and then incubated with a 1000-diluted solution of AP-linked goat antimouse kappa, IgM, or IgG Ab (100 μL/well), respectively, at rt for 1 h. Finally, the plates were washed with PBS and developed with PNPP, followed by colorimetric readout and Ab titer calculations by the methods described above.

Analysis of Cytokines and Chemokines

Concentrations of 20 cytokines/chemokines, including granulocyte-macrophage colony-stimulating factor (GM-CSF), IFN-γ, IL-1α, IL-1β, IL-2, IL-3, IL-4, IL-5, IL-6, IL-9, IL-10, IL-12, IL-13, IL-17, MCP-1, macrophage colony-stimulating factor (M-CSF), RANTES, vascular endothelial growth factor (VEGF), keratinocyte-derived chemokine, and tumor necrosis factor-α, were determined using the Quantibody Mouse Cytokine Array 1 (RayBiotech, USA), according to the manufacturer's instructions. In brief, 100 μL of sample diluent (blocking solution) was added to each well of the microarray of immobilized anticytokine and antichemokine Abs, followed by incubation at rt for 30 min to block nonspecific binding sites and then decantation of the blocking buffer. Thereafter, serially diluted solutions (100 μL) of cytokine standards (concentrations listed in Table S6, Supporting Information) or pooled serum of each group of mice (60 μL, 10 μL from each mouse) were added to each well of the arrays. The arrays were incubated at 4 °C overnight (12 h) and washed 5 times with 150 μL of 1× wash buffer I and 2 times with 150 μL of 1× wash buffer II at rt with gentle shaking. Next, 80 μL of the

https://doi.org/10.1021/jacsau.5c00187
JACS Au 2025, 5, 2210−2222

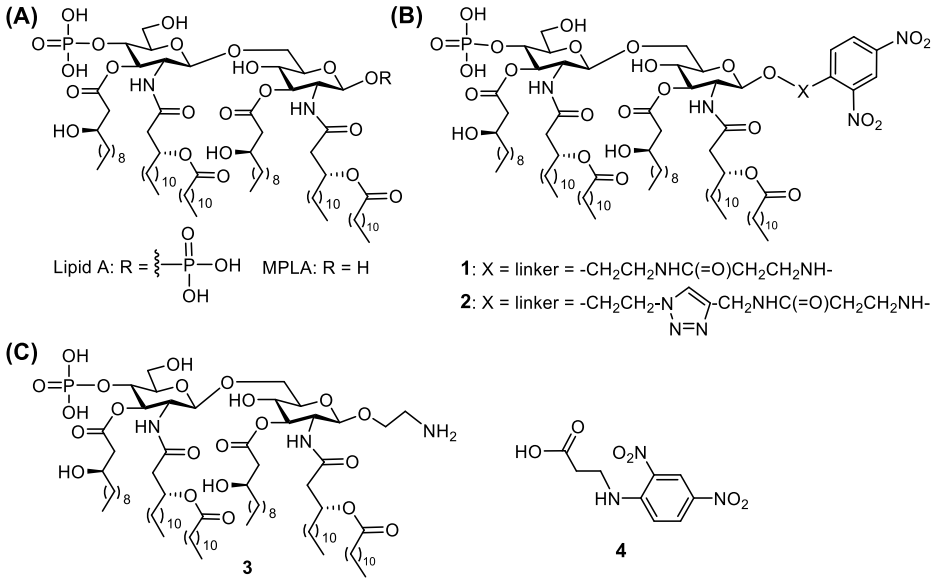

Figure 1. Structures of *N. meningitidis* lipid A and MPLA (A), designed MPLA−DNPA conjugates **1** and **2** with different linkers (B) as new vaccine adjuvants, and MPLA and DNPA derivatives **3** and **4** (C) that were employed as controls.

Scheme 1. Synthesis of the Designed Conjugate Adjuvants 1 and 2

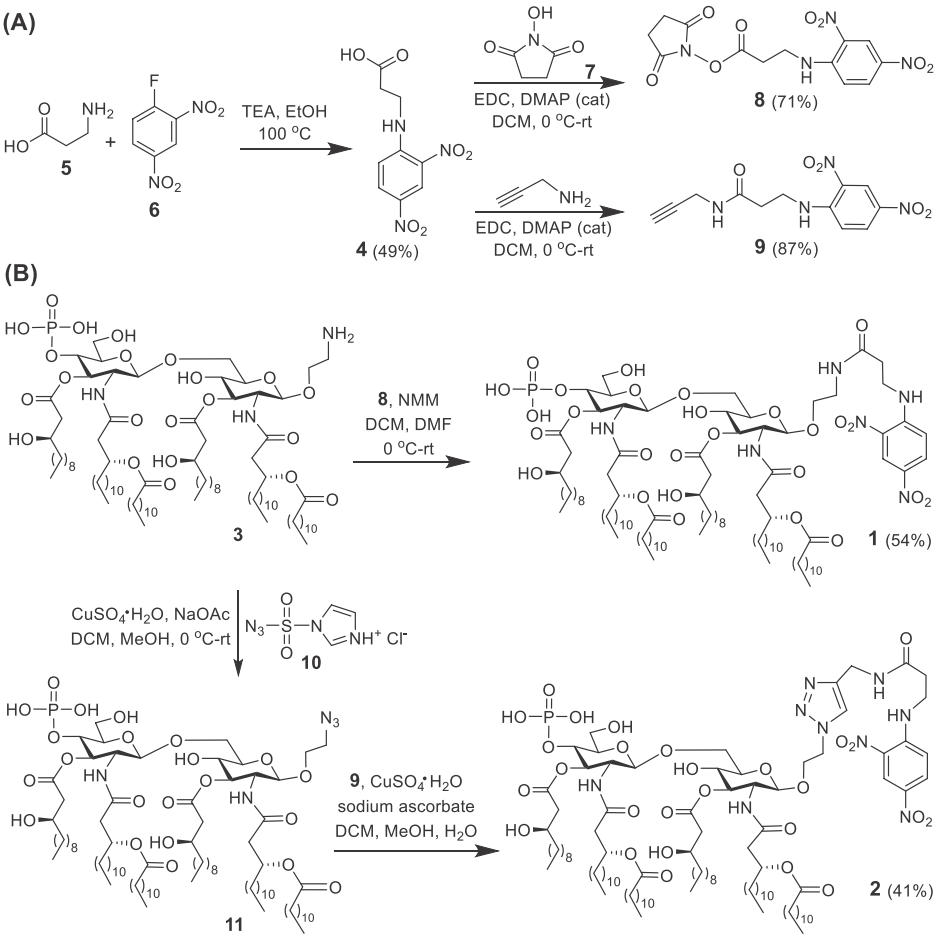

biotinylated detection (secondary) Ab solution was added to each well, and the arrays were incubated at room temperature for 2 h. After the wells were washed as described above, 80 μL of a Cy3-conjugated streptavidin solution was added. The arrays were incubated at rt for 1 h and then washed 5 times with 150 μL of 1× wash buffer I. The arrays were placed in a slide washer/dryer tube, submerged in 30 mL of 1× wash buffer I, gently shaken at rt for 15 min, and washed with 30 mL of 1× wash buffer II. The residual buffer was removed by centrifugation at 1500 rpm for 5 min. Finally, the arrays were sent to

https://doi.org/10.1021/jacsau.5c00187
JACS Au 2025, 5, 2210−2222

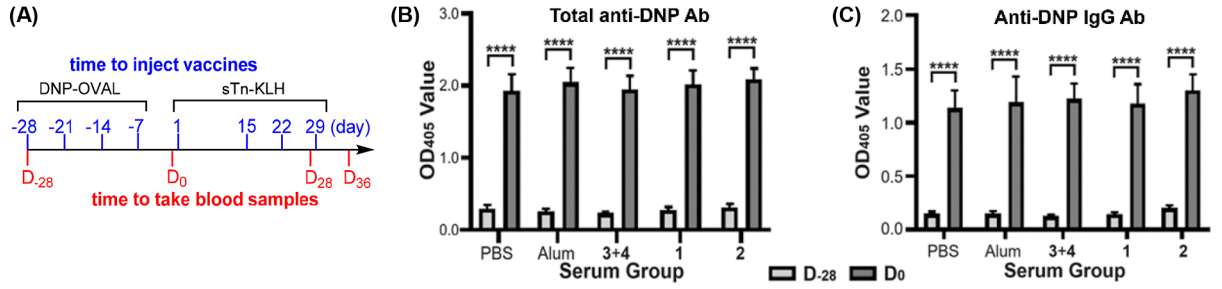

Figure 2. (A) Schedules for mouse inoculation with DNPA−OVAL + alum and sTn−KLH + PBS or an adjuvant, as well as time points to collect blood samples from the mice. (B) Total and (C) IgG anti-DNP Ab levels in the day −28 and day 0 sera (1:50 dilution in PBS buffer) of various groups of mice. Each column represents the mean Ab level for the sera of six mice in a specified group. The error bar indicates the standard error of the mean (SEM). ****$p < 0.0001$ shows the statistical significance level of the difference between two compared groups.

RayBiotech Inc. for scanning and detection, and the data were analyzed by using the RayBiotech cytokine antibody array software.

Statistical Analysis

All data were analyzed by an independent *t*-test between two paired groups using the GraphPad software. $P < 0.05$ is considered statistically significant.

RESULTS AND DISCUSSION

MPLA−DNPA Conjugates as a New Type of Adjuvant

To develop potent and structurally definite adjuvants, MPLA and the DNP motif are attractive lead structures. First, both are potent immunostimulators. Second, they have defined structures and characterized action mechanisms to enable SAR studies. Third, they have different action mechanisms; thus, conjugating them is not likely to hinder their functions. MPLA is the 1-*O*-dephosphoryl derivative of bacterial lipid A (Figure 1A), which elicits both innate and adaptive immune responses[24] via interacting with Toll-like receptor 4 (TLR4) on dendritic cells (DCs) and other immune cells[25] to elicit cytokine and chemokine release, boost immune cell proliferation, enhance antigen presentation, activate Th cells, and stimulate cytotoxic T cells (CTLs).[26−30] The excellent immunological properties of MPLA[31] render it a potent adjuvant and carrier molecule[32−36] for developing and formulating antimicrobial[37−40] and anticancer[41−46] vaccines. The DNP motif is highly immunogenic; thus, natural anti-DNP antibodies (Abs) are abundant in the human serum.[47] The DNP motif provokes the human immune system via recruiting endogenous anti-DNP Abs[48] that can interact with the Fc receptor on DCs and other immune cells to stimulate the Ab effector function.[49−53] Therefore, the DNP motif and endogenous anti-DNP Abs are actively pursued in developing innovative adjuvants and immunotherapies.[54−62]

MPLA and the DNP motif target different pathways to stimulate the human immune system; thus, we expect that their conjugation will harness the immunostimulatory activities of both to result in more potent adjuvants. Moreover, the covalent linkage of MPLA and DNPA may also provide a synergistic effect, as this design will ensure the colocalization of MPLA and the DNP motif on/in the same immune cells to synchronize their actions.[63] To validate the hypothesis and develop more potent adjuvants, we designed and synthesized MPLA−DNPA conjugates **1** and **2** that have different linkers between MPLA and DNPA (Figure 1B), immunologically studied them in mice, and compared them to alum and a mixture of MPLA and DNPA (**3** + **4**, Figure 1C). These studies will reveal the adjuvant activities of designed conjugates and the influences of the linker on their properties. MPLA in **1** and **2** is derived from the lipid A of *Neisseria meningitidis*. SAR studies of lipid A and MPLA in the literature[64−68] and by our group[40,69] demonstrate that this MPLA is not only potent but also consistent as an adjuvant.

Synthesis of Designed Conjugates 1 and 2

The synthesis of **1** and **2** (Scheme 1) commenced with the preparation of 3-(2,4-dinitrophenylamino)propanoic acid **4** and DNPA derivatives **8** and **9** (Scheme 1A)—the key intermediates for synthesizing all MPLA−DNPA conjugates. Compound **4** was also used as a control in an immunological study. Nucleophilic aromatic substitution reactions of 2,4-dinitrophenylfluoride **6** and **5** in the presence of triethylamine (TEA) afforded **4**, which is the common precursor for **8** and **9**. The reaction between **4** and *N*-hydroxysuccinimide (NHS) **7** with 1-ethyl-3-(3-(dimethylamino)propyl)-carbodiimide (EDC) as the condensation reagent provided NHS-activated ester **8** in a 71% yield. Compound **9** was derived from **4** and propargylamine in an 87% yield under the same condition.

MPLA derivative **3** with a free amino group at the glycan reducing end was applied for coupling with **8** and **9** to form MPLA−DNPA conjugates **1** and **2** (Scheme 1B), while **3** was also used as a control in an immunological study. Compound **3** was derived from D-glucosamine by a reported method.[40,69] A chemoselective reaction between amine **3** and activated ester **4** in the presence of *N*-methylmorpholine (NMM) went smoothly to give the desired conjugate **1** in a good yield, which was purified with a silica gel column and then an LH-20 gel filtration column. In the synthesis of conjugate **2**, to facilitate the conjugation of **3** with **9** by click chemistry, we first converted **3** into azide **11** via a diazo transfer reaction with **10** using 1% $CuSO_4{\cdot}5H_2O$ as the catalyst and sodium acetate as the base. Crude product **11** was directly applied for the click reaction with DNPA−alkyne **9** using 1% $CuSO_4{\cdot}5H_2O$ and sodium ascorbate as the catalyst to give conjugate **2** in a 41% yield over two steps after purification with silica gel and LH-20 columns. Conjugates **1** and **2**, as well as all intermediates, were fully characterized with ^1H and ^{13}C NMR and high-resolution MS data. The purities of **1** and **2**, as determined by HPLC, were >91%. Finally, **1**, **2**, and the **3** + **4** mixture were subjected to immunological studies.

Immunological Studies of Conjugate Adjuvants 1 and 2

These in vivo studies were conducted with female C57BL/6J mice, which have an immune system similar to that of humans and, thus, are widely used to study adjuvants and vaccines. Mice were randomly assigned into 5 groups (6 mice/group) and then inoculated with a model vaccine formulated with PBS

https://doi.org/10.1021/jacsau.5c00187
JACS Au 2025, 5, 2210−2222

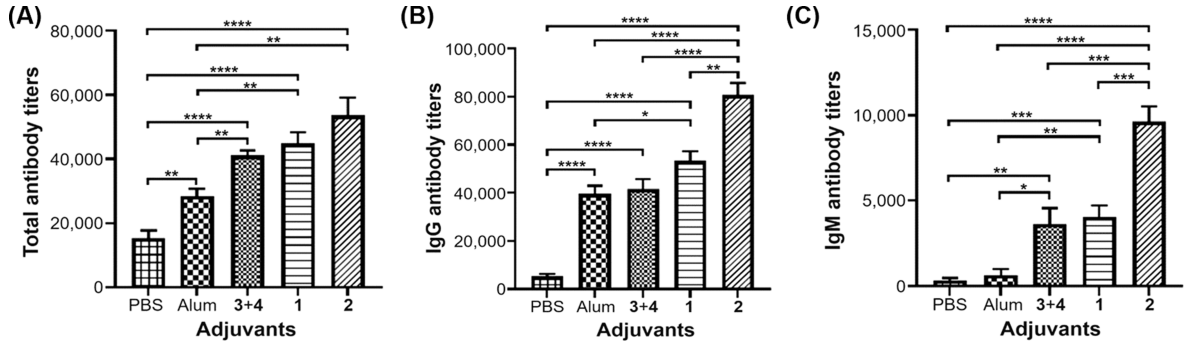

Figure 3. ELISA results of anti-KLH total (A), IgG (B), and IgM (C) Ab titers in the day 36 antisera of mice vaccinated with sTn−KLH combined with PBS, alum, **3** + **4**, **1**, and **2**, respectively. Each column represents the mean Ab titer for a specific group in three parallel experiments. The error bar shows SEM *p < 0.05, **p < 0.01, ***p < 0.001, and ****p < 0.0001, which indicate the statistical significance level of difference between two compared groups.

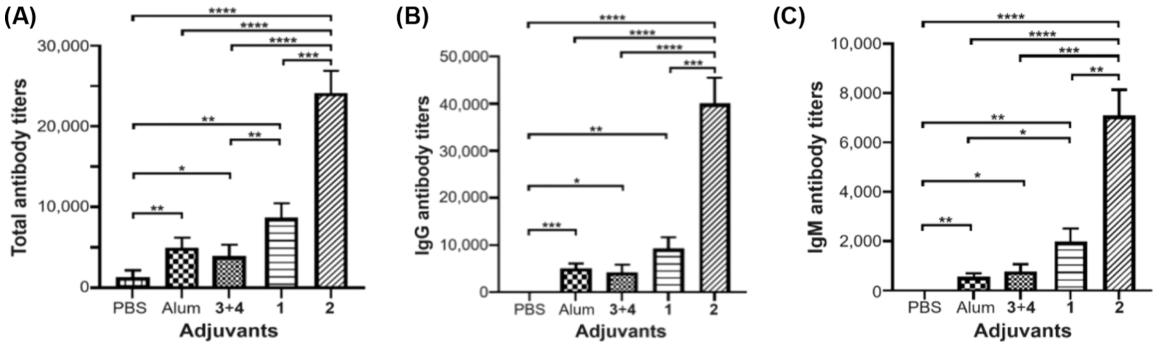

Figure 4. ELISA results of sTn-specific total (A), IgG (B), and IgM (C) Ab titers in the day 36 antisera of mice vaccinated with sTn−KLH combined with PBS, alum, **3** + **4**, **1**, and **2**, respectively. Each column represents the mean titer for a specific group of three parallel experiments. The error bar shows the SEM. *p < 0.05, **p < 0.01, ***p < 0.001, and ****p < 0.0001 indicate the statistical significance level of difference between two compared groups.

(negative control), a **3** + **4** mixture (MPLA + DNPA, a positive control), alum—presently the most used adjuvant (another positive control), and **1** or **2** (tested adjuvants), respectively. Before vaccination, we first inoculated the mice with the commercial DNPA−ovalbumin conjugate (DNPA−OVAL) to induce anti-DNP Abs, as we found that the naïve mice did not contain a significant level of anti-DNP Abs, although high levels of native anti-DNP Abs are present in the human serum.[47] The schedules to inoculate mice with DNPA−OVAL and sTn−KLH, respectively, as well as the time points to collect blood samples from the mice, are presented in Figure 2A.

Enzyme-linked immunosorbent assay (ELISA) results of the day −28 (D_{-28}) sera, the day prior to DNPA−OVAL inoculation, indicate that naïve mice do not express significant levels of anti-DNP Abs. ELISA results of D_0 sera, the day after DNPA−OVAL inoculation 4 times but prior to vaccination with sTn−KLH, indicate that all groups of mice produced similarly high levels of anti-DNP total and IgG Abs upon DNPA−OVAL inoculations (Figure 2B,C). The OD at 405 nm wavelength for anti-DNP IgM Abs also increased (Figure S1A, Supporting Information), but less than that of total and IgG Abs. Nonetheless, these results verify that after DNPA−OVAL inoculation, mice show high levels of anti-DNP Abs and can be used to mimic the human immune system to evaluate MPLA−DNPA conjugates and their immunological properties.

After the mice were provoked to express anti-DNP Abs, they were immunized with a model vaccine formulated with PBS or one of the adjuvants described above. The model vaccine was an sTn−KLH conjugate (8.8% sTn loading), which served as a bifunctional vaccine to test immune responses to both KLH (a protein antigen) and sTn (a poorly immunogenic TACA). The vaccine was combined with alum as an emulsion following the manufacturer's instructions or with **3** + **4**, **1**, or **2** as liposomes formulated with 1,2-distearoyl-*sn*-glycero-3-phosphocholine (DSPC) and cholesterol (2:13:10) according to a reported protocol.[46] These liposomes have an average pore size of 100−200 nm and relatively large polydispersity (PD, index 0.36−0.42; Figures S2−S4, Supporting Information) because they were not subjected to extrusion treatments. Each group of mice was vaccinated via subcutaneous (s.c.) injection of a vaccine preparation (0.1 mL) containing ca. 8 μg of sTn on days 1, 15, 22, and 29, respectively. Blood samples were collected from each mouse on day 0 before vaccination (the blank) and on days 28 and 36, respectively, after vaccination. Antisera were prepared from blood samples by conventional protocols. Antigen-specific Ab levels in the antisera were determined by ELISA, employing KLH and an sTn−human serum albumin (HSA) conjugate as the capture reagents to detect KLH- and sTn-specific Abs, respectively. Total, IgG, and IgM Abs were individually assayed using alkaline phosphatase (AP)-linked goat antimouse kappa, IgG, and IgM secondary Abs. Ab titers were calculated based on the OD value vs serum dilution number plots and defined as the serum dilution numbers corresponding to an OD value of 0.1.

ELISA results of the day 36 antisera using KLH as a capture reagent (Figure 3, and Table S1 of Supporting Information) show that all of the tested adjuvants, including alum, **3** + **4**, **1**,

https://doi.org/10.1021/jacsau.5c00187
JACS Au 2025, 5, 2210−2222

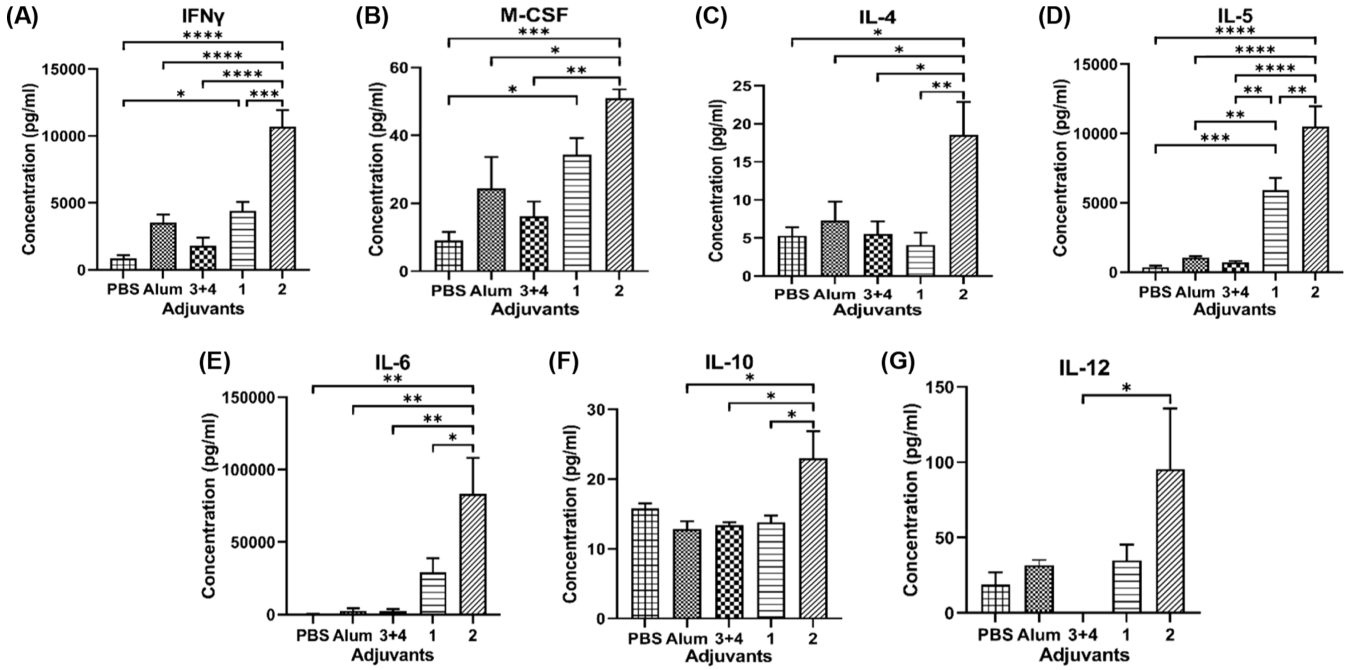

Figure 5. Concentrations of IFN-γ (A), M-CSF (B), IL-4 (C), IL-5 (D), IL-6 (E), IL-10 (F), and IL-12 (G) in the pooled day 38 antisera from mice immunized with sTn−KLH plus PBS or an adjuvant, such as alum, **3 + 4**, **1**, and **2**. Each column represents the mean for a specific group of mice in triplicate experiments, and the error bar indicates the SEM. *p < 0.05, **p < 0.01, ***p < 0.001, and ***p < 0.001 show the statistical significance level for the difference between two compared groups.

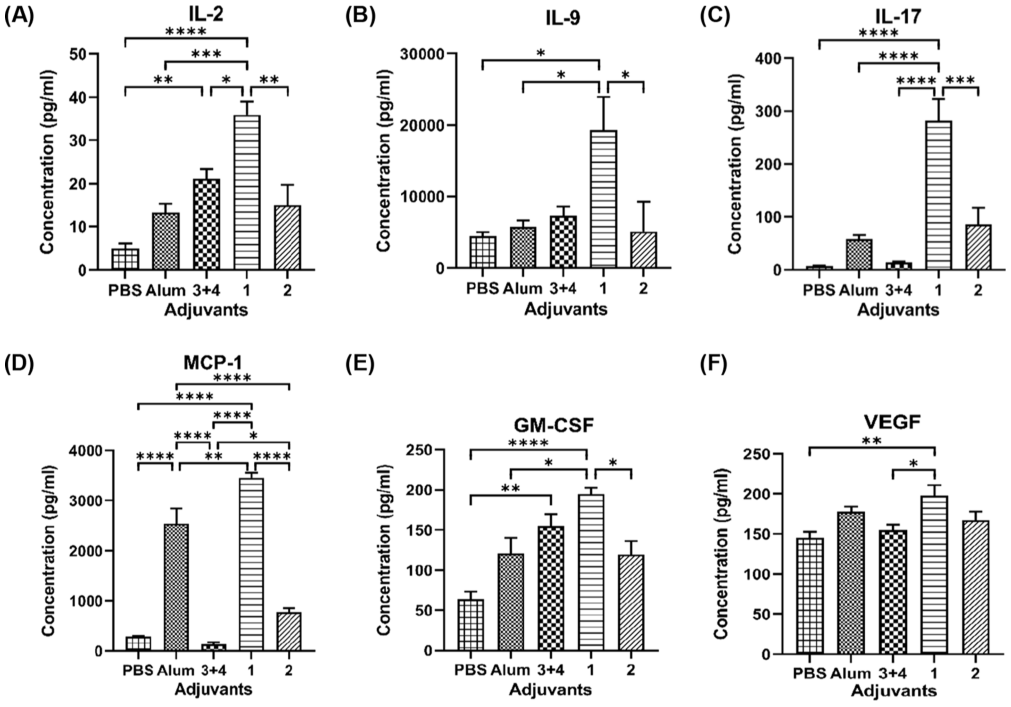

Figure 6. Concentrations of IL-2 (A), IL-9 (B), IL-17 (C), MCP-1 (D), GM-CSF (E), and VEGF (F) in the pooled day 38 antisera from mice immunized with sTn−KLH plus PBS or an adjuvant including alum, **3 + 4**, **1**, and **2**. Each column represents the mean for a specific group of mice in triplicate experiments, and the error bar indicates the SEM *p < 0.05, **p < 0.01, ***p < 0.001, and ***p < 0.001 show the statistical significance level for the difference between two compared groups.

and **2**, helped sTn−KLH elicit anti-KLH immune responses, reflected by higher anti-KLH total Ab titers in these groups than that in the PBS group (Figure 3A). Additionally, the Abs were mainly of IgG type (Figure 3B), and significant levels of IgM Abs were also observed with **3 + 4**, **1**, and **2** as adjuvants (Figure 3C). These results further verify that **3 + 4**, **1**, and **2**, especially the latter, are better adjuvants than alum—the positive control. Under the influence of conjugate **2**, the vaccine stimulated the strongest anti-KLH IgG (Figure 3B) and IgM (Figure 3C) Ab responses, and the differences of this

https://doi.org/10.1021/jacsau.5c00187
JACS Au 2025, 5, 2210−2222

group of mice from all other groups were statistically very significant ($p < 0.01$).

ELISA studies of the day 36 antisera with sTn−HSA as capture antigen disclose the anti-sTn Ab profile (Figure 4 and Table S2 of the Supporting Information), which is similar to that of anti-KLH Abs in certain aspects. For example, all adjuvants, alum, **3** + **4**, **1**, and **2**, helped sTn−KLH stimulate robust anti-sTn total (Figure 4A), IgG (Figure 4B), and IgM (Figure 4C) Abs, as opposed to PBS. However, while the anti-sTn Ab levels for alum and **3** + **4** are similar, **1** elicited a slightly stronger anti-sTn Ab response than alum. More importantly, **2** helped sTn−KLH elicit much higher levels of anti-sTn total, IgG, and IgM Abs than other adjuvants, including conjugate **1**.

Our immunological studies have been focused on antisera obtained from mice after the fourth immunization because this is the final one, and we can prepare large quantities of terminal antisera to meet the demand from various analyses. However, we also analyzed the day 28 (a week after the third vaccination) antisera, revealing high levels of anti-KLH and -sTn IgG Abs (Figure S5 and Table S3, Supporting Information). These results suggest the successful vaccination of mice after 3 times of immunization. Similarly, conjugate **2** is also better than others to help elicit Abs, especially against sTn. Although the day 36 antisera showed higher Ab levels than the day 28 antisera, suggesting the enhancement of immune responses after each boost vaccination (which is anticipated), they exhibited the same pattern and thus should give the same conclusion. The high IgG Ab levels also suggest the development of T/Th cell-mediated robust, long-term, and memorable immunity against the vaccine under the influence of **1** and **2**, further validating the efficacy of these new vaccine adjuvants.

To gain more insight into the adjuvanting mechanism of MPLA−DNPA conjugates, we compared the cytokines/chemokines produced by various groups of mice. Therefore, each group of antisera was pooled and applied to a commercial microarray, according to the manufacturer's instructions. The expression levels of 20 cytokines and chemokines were quantified by the array provider. It is shown that interferon (IFN)-γ, M-CSF, interleukin (IL)-4, IL-5, IL-6, and IL-12 are upregulated in adjuvant **2** group (Figure 5 and Table S4 of Supporting Information) when compared to **1** and other groups. These cytokines and chemokines play a critical role in regulating the immune system, e.g., activation and proliferation of macrophage, B, T, natural killer (NK), and other immune cells, T cell differentiation into Th1/Th2 cells, stimulation of CD8+ CTLs and major histocompatibility complex class II (MHC-II) molecules, enhanced antigen presentation, Ab production, isotype switch, etc., to stimulate T cell-mediated immunity. Hence, the increased immune response to sTn−KLH in the presence of **2** can be related to the production of a wide range of cytokines and chemokines.

Our results further reveal the overexpression of IL-2, IL-9, IL-17, and monocyte chemoattractant protein-1 (MCP-1) in the adjuvant **1** group as compared to other groups (Figure 6A−D and Table S4 of the Supporting Information). The GM-CSF level in the adjuvant **1** group is also higher than that in the PBS, alum, and adjuvant **2** groups, but its difference from the **3** + **4** group is not statistically significant (Figure 6E, and Table S4 of Supporting Information). In the **1** group, a higher level of IL-5 than all control groups (Figure 5D) and higher levels of IFN-γ, M-CSF (Figure 5A,B), VEGF (Figure 5F), IL-1β, IL-3, and normal T expressed and secreted (RANTES) than the PBS group (Figure S6A−C and Table S4, Supporting Information) were also observed. These cytokines/chemokines can elicit CD4+ and CD8+ T cell proliferation and function, stimulate Ab production, support Th cell growth, and regulate monocyte, macrophage, DC, memory T lymphocyte, and NK cell migration and infiltration, thereby modulating both innate and adaptive immunities. The collective actions of these cytokines and chemokines can be responsible for the adjuvant properties of **1**. However, **1** and **2** elicited different cytokines and chemokines.

In contrast, alum leads to the overexpression of IL-1β, IL-3, and RANTES (Figure S6A−C and Table S4, Supporting Information), as well as a higher level of MCP-1, than PBS (Figure 6D), while the mice in the **3** + **4** group only expressed higher levels of IL-2 and GM-CSF compared to mice in the PBS group (Figure 6A,E). The results are consistent with the relatively weak adjuvant activities observed for alum and **3** + **4** as compared to **1** and **2**.

Discussion of the Immunological Results

Our results show that all tested adjuvants, including alum, **3** + **4**, **1**, and **2**, boost immune responses against both KLH and sTn of model vaccine sTn−KLH (Figures 3 and 4). This is expected, as alum and MPLA (e.g., **3**) are well-established adjuvants, and **1** and **2** are based on MPLA and, thus, should possess adjuvant activities. In addition, overall, the anti-KLH IgG and IgM Ab titers are higher than the corresponding anti-sTn Ab titers, which agrees with the conventional paradigm; i.e., protein antigens are typically more immunogenic than carbohydrate antigens. Moreover, all adjuvants helped the vaccine provoke robust IgG Ab responses against KLH and sTn (Figures 3B and 4B), indicating Ab isotype switch and maturation and, therefore, cellular immunity, which is desired for effective vaccination.[70]

ELISA results in Figure 3 demonstrate that alum and **3** + **4** possess similar efficacies to boost IgG Ab responses against KLH (Figure 3B), but the **3** + **4** group shows higher levels of IgM and total Abs than the alum group. Thus, **3** + **4** is slightly more effective than alum in eliciting innate immunity to protein antigen KLH, while they have similar potencies to elicit adaptive immunities. In contrast, **1** and **2** exhibit significantly stronger adjuvant activity than alum, in terms of both total and IgG Abs against KLH. Moreover, **2** is much more potent than **3** + **4** (Figure 3B,C), and **1** is slightly more potent than **3** + **4**. The results indicate that conjugating MPLA and DNPA leads to improved adjuvant activity. Significantly, **2** is much more potent than **1** (Figure 3B,C), which are structurally different only in the linker. A potential reason for the increased activity of **1** and **2** over alum is their incorporation into liposomes, which should facilitate multivalent presentation for more efficient B-cell immunoglobulin (Ig) receptor clustering and enhanced immunological activities.[71−74] However, this cannot explain why **2** and **1** are much more potent than **3** + **4**. A plausible explanation for the enhanced immunological activities of **2** and **1** over alum and **3** + **4** is a synergistic effect of MPLA and DNPA in the conjugates, and also, a minimal distance between MPLA and DNP within the conjugate is required for their efficient interaction with specific targets on immune cells to exhibit the synergistic effect. Therefore, the linker has a big impact on the adjuvant activity, and **2** is more potent than **1**.

https://doi.org/10.1021/jacsau.5c00187
JACS Au 2025, 5, 2210−2222

The ELISA results of anti-sTn Abs (Figure 4) provide additional and more striking support for the above conclusion. Again, alum and **3** + **4** are comparable in promoting anti-sTn total, IgG, and IgM Abs, whereas conjugates **1** and **2** show adjuvant activities stronger than those of alum and **3** + **4**. Most significantly, **2** is much more potent than both **3** + **4** and **1** to help elicit anti-sTn total, IgG, and IgM Abs, and this difference is much more evident than the difference among the anti-KLH Abs. The results suggest a greater synergistic effect between DNPA and MPLA in **2** as an adjuvant for the sTn antigen and a greater impact of the linker on the synergistic effect. Thus, the MPLA−DNPA conjugates as adjuvants may significantly benefit carbohydrate vaccines.

The cytokine and chemokine profiles in various groups of mice are consistent with the ELISA results and provide more insights into the immune response. Conjugate **2** results in upregulations of IFN-γ, M-CSF, IL-4, IL-5, IL-6, and IL-12 (Figure 5). IFN-γ produced by NK and NKT cells in innate immunity and by CD4+ Th1 and CD8+ CTL effector T cells in antigen-specific immunity[75] plays a critical role in macrophage activation and MHC-II molecule expression to enhance antigen presentation.[76] It is also an important mediator of the Ab isotype switch and CD8+ CTL differentiation, activation, and proliferation.[77,78] A major function of M-CSF is to regulate monocyte and macrophage proliferation, differentiation, and activation.[79,80] IL-4 upregulation is indicative of Th2 cell activation[81] to promote naive CD4+ T cell polarization into Th2 cells,[82] which produce IL-4, IL-5, and IL-13.[83] Th2 cells are important in providing T cell support to B cells to facilitate Ab production and class switch to IgG1 and effector T cell immune responses.[84] IL-4 also promotes activated B and T cell proliferation.[83] IL-5 induces B cell growth and Ig secretion.[85,86] IL-6 is produced by monocytes, macrophages, and T cells[87] in response to pathogen-associated molecular patterns that bind a group of detection molecules of the innate immune system, known as pattern recognition receptors, such as TLRs.[88,89] Thus, IL-6 overexpression potentially indicates MPLA involvement in immunity. The main functions of IL-10 are to downregulate Th1 cytokine and MHC-II molecule expression and enhance B cell survival, proliferation, and Ab production.[90,91] IL-12, expressed by several immune cells in response to antigenic stimulation,[92,93] plays a key role in enhancing the cytotoxic activity of NK cells and CD8+ CTLs[94,95] via stimulating T cell growth and functions and reducing IL-4-mediated IFN-γ suppression.[93] Elevated IL-12 suggests NK cell activation[96] and differentiation of naïve T cells into Th1 cells.[95]

It is also disclosed that **1** results in IL-2, IL-9, IL-17, and MCP-1 overexpression (Figure 6A−D), as well as a higher level of GM-CSF, than that of PBS, alum, and **2** (Figure 6E). IL-2[97] is a proliferative signal for DCs and T or NK cells[98] to promote CD4+ and CD8+ T cell proliferation and function.[99,100] It also promotes B cell proliferation and Ab production.[101−103] IL-9 is produced by Th2 and Th9 cells to regulate IL-2/IL-4-independent Th cell growth and Ig production.[104−106] IL-17 is secreted by activated CD4+ cells, memory CD8+ T cells, as well as other immune cells[107] to elicit immunity via elevating neutrophil recruitment and antimicrobial peptide production, and is involved in innate and adaptive immunity.[108] MCP-1 modulates monocyte, macrophage, DC, memory T lymphocyte, and NK cell migration and infiltration to the site of inflammation in infection, etc.[109,110] GM-CSF is expressed by several cell types, e.g., macrophages and T, mast, and NK cells, to boost cell proliferation, maturation, and survival.[111,112] Additionally, **1** also results in IL-5 overexpression compared to all controls (Figure 5D), as well as higher levels of IFN-γ, M-CSF (Figure 5A,B), VEGF (Figure 6F), IL-1β, IL-3, and RANTES (Figure S6A−C, Supporting Information) than PBS. IL-1β is a potent pro-inflammatory cytokine in response to pathogens.[113] IL-3 is produced by distinct subsets of T and mast cells and basophils, and it is involved in inflammation and tumor-associated angiogenesis.[114,115] RANTES is produced by CD8+ T cells, platelets, and epithelial cells to play a critical role in supporting T cell functions and recruiting immune cells to the site of inflammation.[116,117]

The cytokine/chemokine profiles associated with **1** and **2** suggest that they can enhance both innate and adaptive immunities toward vaccines. However, alums **1**, **2**, and **3** + **4** elicit different cytokines and chemokines, indicating potentially different modes of action and the impact of linkers in conjugate adjuvants **1** and **2** on their immunological activities. Overall, **1** and **2** boost T cell-mediated cellular immunity via enhancing macrophage, DC, B, T, NK, and other immune cell proliferation and activation and promoting T cell differentiation into Th1/Th2 cells, MHC-I/II molecule expression, antigen presentation, cytokine secretion, and Ab production and isotype switch. The wide scope of cytokines and chemokines elicited by **2** is consistent with its strong adjuvant activity and indicates its broad interaction with the immune system.

These results strongly support the synergistic effect of covalently linked MPLA and DNPA, especially in compound **2**. Although more studies are necessary to elucidate the exact immunological mechanisms for this synergy, current cytokine and chemokine profiles and previous findings on glycoconjugate vaccines[118] suggest that conjugating MPLA and DNPA may ensure their colocalization on the same immune cells to provide the opportunity for them to act in synergy in boosting antigen processing by professional antigen-presenting cells (such as DCs), antigenic epitope presentation by MHC-I/II molecules, activation and proliferation of immune cells, and other immunological activities, thereby promoting immune responses to vaccines.[119] As indicated in Figure 7, both MPLA and DNPA can activate DCs via interacting with TLR4 and recruiting endogenous anti-DNP Abs to interact with Fc receptors, respectively,[120,121] in a cis or trans manner (interacting with targets on the same or opposite cells, respectively). The synergistic actions of MPLA and DNPA on DCs and other immune cells can enhance antigen presentation and T cell involvement in responding to a vaccine, thus promoting T cell immunity (Figure 7).[121] This model explains not only the increased activities of MPLA−DNPA conjugates over **3** + **4** but also the difference between **1** and **2**, since the concurrent binding of MPLA and DNPA in these conjugates with specific targets on the same or different cells requires a proper distance between the two epitopes, as reflected by the influence of the linker on their activities. Clearly, **2** with a longer linker is much more potent than analogous **1** with a shorter linker, which can be attributed to the increased flexibility of the former to facilitate its bifunctional interaction with immune cells. However, whether the linker in **2** is optimal or not for this type of conjugate adjuvant remains unknown, which will be answered through more SAR studies in the future. Moreover, presently, we cannot eliminate another potential but less likely explanation for the increased activity of

https://doi.org/10.1021/jacsau.5c00187
JACS Au 2025, 5, 2210−2222

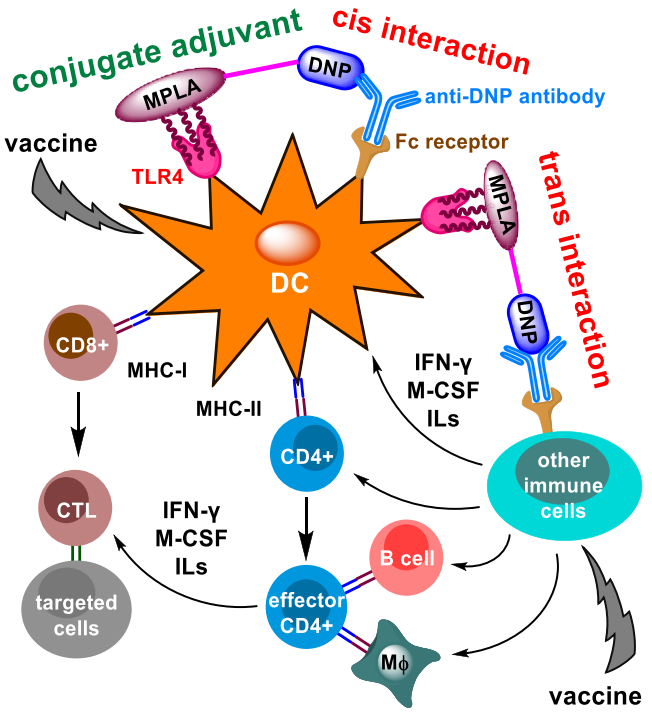

Figure 7. Proposed mode of action for the synergistic effect of DNP and MPLA in conjugate adjuvants. MPLA and recruited endogenous anti-DNP Abs interact with TLR4 and Fc receptors, respectively, on DCs and other immune cells to act in synergy to boost antigen processing/presentation and Th, T and B cell activation, thereby promoting T cell-mediated adaptive immunity against vaccines.[121] Bifunctional interactions between MPLA–DNPA conjugates and immune cells can be cis or trans.

2 over **1**, i.e., the triazole moiety in **2** can also elicit Abs, which may have a similar function as the endogenous anti-DNP Abs. This question can be answered in the future via preparing an MPLA–DNPA conjugate with a linker of similar length as in **2** and comparing the two conjugates.

CONCLUSIONS

In this work, we synthesized and studied MPLA–DNPA conjugates as a new type of vaccine adjuvant. The immunological results reveal that MPLA–DNPA conjugates **1** and **2** are more potent than alum (Figures 3 and 4). Importantly, **1** and **2** help boost robust immune responses to the model vaccine sTn–KLH against both its protein antigen KLH and carbohydrate antigen sTn. In both cases, the IgG Ab response is strong, indicating Ab isotype switch and affinity maturation, thereby T cell involvement in the immunity, which is verified by in-depth analysis of the elicited cytokines and chemokines. The results also suggest that **1** and **2** can help boost adaptive and long-term memorable immunities. More interestingly, **1** and **2** are much stronger than a mixture of MPLA and DNPA. In addition, conjugate **2** is more potent than **1**, which are structurally different only in terms of their linkers between MPLA and DNPA, and **2** can help provoke extremely robust anti-sTn Ab responses. The results, together with a wider scope of cytokines/chemokines elicited by **2** compared to other adjuvants, suggest a synergistic effect of the immunostimulatory activities of MPLA and DNPA in the covalently conjugated form and an impact of the linker, which may affect the concurrent binding of MPLA and anti-DNP Ab with their specific receptors, on the immunological property of the resulting conjugates. As a result, conjugate **2** is identified as a promising adjuvant, particularly for carbohydrate vaccines, which is worthy of further research and development. Subsequently, we will prepare and systematically study MPLA–DNPA conjugates with varied linkers to find the best adjuvant. We will also investigate the applications of these conjugate adjuvants to other vaccines and gain more insights into their functional mechanisms to facilitate their further improvement and the design of other conjugate adjuvants.

ASSOCIATED CONTENT

Data Availability Statement

The data underlying this study are available in the published article and its Supporting Information.

Supporting Information

The Supporting Information is available free of charge at https://pubs.acs.org/doi/10.1021/jacsau.5c00187.

NMR and MS data and spectra of all new compounds and additional data of immunological studies (PDF)

AUTHOR INFORMATION

Corresponding Author

Zhongwu Guo – *Department of Chemistry, University of Florida, Gainesville, Florida 32611, United States; UF Health Cancer Center, University of Florida, Gainesville, Florida 32611, United States;* orcid.org/0000-0001-5302-6456; Email: zguo@chem.ufl.edu

Authors

Jiatong Guo – *Department of Chemistry, University of Florida, Gainesville, Florida 32611, United States*

Rajendra Rohokale – *Department of Chemistry, University of Florida, Gainesville, Florida 32611, United States*

Sayan Kundu – *Department of Chemistry, University of Florida, Gainesville, Florida 32611, United States;* orcid.org/0000-0003-0628-6698

Complete contact information is available at: https://pubs.acs.org/10.1021/jacsau.5c00187

Author Contributions

§J.G. and R.R. contributed equally. The manuscript was written through contributions from all authors. All authors have given approval to the final version of the manuscript.

Funding

This work is supported by a research grant (R21 AI170129) from NIH/NIAID. The MS instrument was supported by NIH grants S10 OD021758 and S10 OD030250.

Notes

The authors declare no competing financial interest.

ACKNOWLEDGMENTS

Z.G. is grateful to Drs. Steven and Rebecca Scott for their endowment to support the research.

REFERENCES

(1) Hollingsworth, R. E.; Jansen, K. Turning the corner on therapeutic cancer vaccines. *npj Vaccines* **2019**, *4*, 7.

(2) Antonarelli, G.; Corti, C.; Tarantino, P.; Ascione, L.; Cortes, J.; Romero, P.; Mittendorf, E. A.; Disis, M. L.; Curigliano, G.

Therapeutic cancer vaccines revamping: Technology advancements and pitfalls. *Ann. Oncol.* **2021**, *32*, 1537−1551.
(3) Kaczmarek, M.; Poznańska, J.; Fechner, F.; Michalska, N.; Paszkowska, S.; Napierała, A.; Mackiewicz, A. Cancer vaccine therapeutics: Limitations and effectiveness-a literature review. *Cells* **2023**, *12*, 2159.
(4) Liu, J.; Fu, M.; Wang, M.; Wan, D.; Wei, Y.; Wei, X. Cancer vaccines as promising immuno-therapeutics: Platforms and current progress. *J. Hematol. Oncol.* **2022**, *15*, 28.
(5) Lin, M. J.; Svensson-Arvelund, J.; Lubitz, G. S.; Marabelle, A.; Melero, I.; Brown, B. D.; Brody, J. D. Cancer vaccines: the next immunotherapy frontier. *Nat. Cancer* **2022**, *3*, 911−926.
(6) Awate, S.; Babiuk, L. A.; Mutwiri, G. Mechanisms of action of adjuvants. *Front. Immunol.* **2013**, *4*, No. e114.
(7) Pulendran, B.; Ahmed, R. Immunological mechanisms of vaccination. *Nat. Immunol.* **2011**, *12*, 509−517.
(8) Shi, S.; Zhu, H.; Xia, X.; Liang, Z.; Ma, X.; Sun, B. Vaccine adjuvants: Understanding the structure and mechanism of adjuvanticity. *Vaccine* **2019**, *37*, 3167−3178.
(9) O'Hagan, D. T.; Fox, C. B. New generation adjuvants–from empiricism to rational design. *Vaccine* **2015**, *33*, B14−B20.
(10) Wilson-Welder, J. H.; Torres, M. P.; Kipper, M. J.; Mallapragada, S. K.; Wannemuehler, M. J.; Narasimhan, B. Vaccine adjuvants: current challenges and future approaches. *J. Pharm. Sci.* **2009**, *98*, 1278−1316.
(11) Petrovsky, N.; Aguilar, J. C. Vaccine adjuvants: Current state and future trends. *Immunol. Cell Biol.* **2004**, *82*, 488−496.
(12) Kaisho, T.; Akira, S. Toll-like receptors as adjuvant receptors. *Biochim. Biophys. Acta* **2002**, *1589*, 1−13.
(13) De Gregorio, E.; Caproni, E.; Ulmer, J. B. Vaccine adjuvants: Mode of action. *Front. Immunol.* **2013**, *4*, 214.
(14) Shah, R. R.; Hassett, K. J.; Brito, L. A. Overview of vaccine adjuvants: Introduction, history, and current status. In *Vaccine Adjuvants: Methods and Protocols*; Fox, C. B., Ed.; Humana Press: New York, 2017; pp 1−14.
(15) Guimarães, L. E.; Baker, B.; Perricone, C.; Shoenfeld, Y. Vaccines, adjuvants and autoimmunity. *Pharmacol. Res.* **2015**, *100*, 190−209.
(16) Mount, A.; Koernig, S.; Silva, A.; Drane, D.; Maraskovsky, E.; Morelli, A. B. Combination of adjuvants: the future of vaccine design. *Expert Rev. Vaccines* **2013**, *12*, 733−746.
(17) Del Giudice, G.; Rappuoli, R.; Didierlaurent, A. M. Correlates of adjuvanticity: A review on adjuvants in licensed vaccines. *Semin. Immunol.* **2018**, *39*, 14−21.
(18) Pon, R. A.; Jennings, H. J. Carbohydrate-based antibacterial vaccines. In *Carbohydrate-Based Vaccines and Immunotherapies*; Guo, Z., Boons, G.-J., Eds.; John Wiley & Sons, Inc.: Hoboken, 2009; pp 117−166.
(19) Wang, Q.; Ekanayaka, S. A.; Wu, J.; Zhang, J.; Guo, Z. Synthetic and immunological studies of 5′-N-phenylacetyl sTn to develop carbohydrate-based cancer vaccines and to explore the impacts of linkage between carbohydrate antigens and carrier proteins. *Bioconjugate Chem.* **2008**, *19*, 2060−2068.
(20) Guy, B. Adjuvants for protein- and carbohydrate-based vaccines. In *Carbohydrate-Based Vaccines and Immunotherapies*; Guo, Z., Boons, G.-J., Eds.; John Wiley & Sons, Inc.: Hoboken, 2009; pp 89−116.
(21) Batista-Duharte, A.; Martínez, D. T.; Carlos, I. Z. Efficacy and safety of immunological adjuvants. Where is the cut-off? *Biomed. Pharmacother.* **2018**, *105*, 616−624.
(22) Danishefsky, S. J.; Shue, Y.-K.; Chang, M. N.; Wong, C.-H. Development of Globo-H Cancer Vaccine. *Acc. Chem. Res.* **2015**, *48*, 643−652.
(23) Rohokale, R.; Guo, J.; Guo, Z. Monophosphoryl lipid A-rhamnose conjugates as a new class of vaccine adjuvants. *J. Med. Chem.* **2024**, *67*, 7458−7469.
(24) Iwasaki, A.; Medzhitov, R. Toll-like receptor control of the adaptive immune responses. *Nat. Immunol.* **2004**, *5*, 987−995.
(25) Maeshima, N.; Fernandez, R. C. Recognition of lipid A variants by the TLR4-MD-2 receptor complex. *Front. Cell. Infect. Microbiol.* **2013**, *3*, No. e3.
(26) Dobrovolskaia, M. A.; Vogel, S. N. Toll receptors, CD14, and macrophage activation and deactivation by LPS. *Microb. Infect.* **2002**, *4*, 903−914.
(27) Martin, M.; Michalek, S. M.; Katz, J. Role of innate immune factors in the adjuvant activity of monophosphoryl lipid A. *Infect. Immun.* **2003**, *71*, 2498−2507.
(28) Jonuleit, H.; Knop, J.; Enk, A. H. Cytokines and their effects on maturation, differentiation and migration of dendritic cells. *Arch. Dermatol. Res.* **1996**, *289*, 1−8.
(29) Masihi, K. N.; Lange, W.; Johnson, A. G.; Ribi, E. Enhancement of chemiluminescence and phagocytic activities by nontoxic and toxic forms of lipid A. *J. Biol. Response Modif.* **1986**, *5*, 462−469.
(30) Reisser, D.; Pance, A.; Jeannin, J.-F. Mechanisms of the antitumoral effect of lipid A. *BioEssays* **2002**, *24*, 284−289.
(31) Persing, D. H.; Coler, R. N.; Lacy, M. J.; Johnson, D. A.; Baldridge, J. R.; Hershberg, R. M.; Reed, S. G. Taking toll: lipid A mimetics as adjuvants and immunomodulators. *Trends Microbiol.* **2002**, *10*, S32−S37.
(32) Ulrich, J. T.; Cantrell, J. L.; Gustafson, G. L.; Myers, K. R.; Rudbach, J. A.; Hiernaux, J. R. The adjuvant activity of monophosphoryl lipid A. In *Topics in Vaccine Adjuvant Research*; CRC Press, 1991; pp 133−143.
(33) De Becker, G.; Moulin, V.; Pajak, B.; Bruck, C.; Francotte, M.; Thiriart, C.; Urbain, J.; Moser, M. The adjuvant monophosphoryl lipid A increases the function of antigen-presenting cells. *Int. Immunol.* **2000**, *12*, 807−815.
(34) Baldridge, J.; Myers, K.; Johnson, D.; Persing, D.; Cluff, C.; Hershberg, R. Monophosphoryl lipid A and synthetic lipid A mimetics as TLR4-based adjuvants and immunomodulators. In *Vaccine Adjuvants*; Hackett, C. J., Harn, D. A. J., Eds.; Humana Press Inc.: Totowa, NJ, 2006; pp 235−255.
(35) Zhang, Y.; Gaekwad, J.; Wolfert, M. A.; Boons, G.-J. Modulation of innate immune responses with synthetic lipid A derivatives. *J. Am. Chem. Soc.* **2007**, *129*, 5200−5216.
(36) Ingale, S.; Wolfert, M. A.; Buskas, T.; Boons, G. J. Increasing the antigenicity of synthetic tumor-associated carbohydrate antigens by targeting Toll-like receptors. *Chembiochem* **2009**, *10*, 455−463.
(37) Bojang, K. A.; Milligan, P. J.; Pinder, M.; Vigneron, L.; Alloueche, A.; Kester, K. E.; Ballou, W. R.; Conway, D. J.; Reece, W. H.; Gothard, P.; Yamuah, L.; Delchambre, M.; Voss, G.; Greenwood, B. M.; Hill, A.; McAdam, K. P.; Tornieporth, N.; Cohen, J. D.; Doherty, T. Efficacy of RTS,S/AS02 malaria vaccine against Plasmodium falciparum infection in semi-immune adult men in The Gambia: A randomised trial. *Lancet* **2001**, *358*, 1927−1934.
(38) Boland, G.; Beran, J.; Lievens, M.; Sasadeusz, J.; Dentico, P.; Nothdurft, H.; Zuckerman, J. N.; Genton, B.; Steffen, R.; Loutan, L.; Hattum, J. V.; Stoffel, M. Safety and immunogenicity profile of an experimental hepatitis B vaccine adjuvanted with AS04. *Vaccine* **2004**, *23*, 316−320.
(39) Goepfert, P. A.; Tomaras, G. D.; Horton, H.; Montefiori, D.; Ferrari, G.; Deers, M.; Voss, G.; Koutsoukos, M.; Pedneault, L.; Vandepapeliere, P.; McElrath, M. J.; Spearman, P.; Fuchs, J. D.; Koblin, B. A.; Blattner, W. A.; Frey, S.; Baden, L. R.; Harro, C.; Evans, T. Durable HIV-1 antibody and T-cell responses elicited by an adjuvanted multi-protein recombinant vaccine in uninfected human volunteers. *Vaccine* **2007**, *25*, 510−518.
(40) Wang, L.; Feng, S.; Wang, S.; Li, H.; Guo, Z.; Gu, G. Synthesis and immunological evaluation of lipoarabinomannan oligosaccharide-monophosphoryl lipid A conjugates as novel antituberculosis vaccines. *J. Org. Chem.* **2017**, *82*, 12085−12906.
(41) Schultz, N.; Oratz, R.; Chen, D.; Zeleniuch-Jacquotte, A.; Abeles, G.; Bystryn, J.-C. Effect of DETOX as an adjuvant for melanoma vaccine. *Vaccine* **1995**, *13*, 503−508.
(42) Sondak, V. K.; Liu, P. Y.; Tuthill, R. J.; Kempf, R. A.; Unger, J. M.; Sosman, J. A.; Thompson, J. A.; Weiss, G. R.; Redman, B. G.; Jakowatz, J. G.; Noyes, R. D.; Flaherty, L. E. Adjuvant immunotherapy

https://doi.org/10.1021/jacsau.5c00187
JACS Au 2025, 5, 2210−2222

of resected, intermediate-thickness, node-negative melanoma with an allogeneic tumor vaccine: overall results of a randomized trial of the Southwest Oncology Group. *J. Clin. Oncol.* **2002**, *20*, 2058−2066.
(43) Butts, C.; Murray, N.; Maksymiuk, A.; Goss, G.; Marshall, E.; Soulières, D.; Cormier, Y.; Ellis, P.; Price, A.; Sawhney, R.; Davis, M.; Mansi, J.; Smith, C.; Vergidis, D.; Ellis, P.; MacNeil, M.; Palmer, M. Randomized phase IIB trial of BLP25 liposome vaccine in stage IIIB and IV non-small-cell lung cancer. *J. Clin. Oncol.* **2005**, *23*, 6674−6681.
(44) North, S. A.; Graham, K.; Bodnar, D.; Venner, P. A pilot study of the liposomal MUC1 vaccine BLP25 in prostate specific antigen failures after radical prostatectomy. *J. Urol.* **2006**, *176*, 91−95.
(45) Zhou, Z.; Mandal, S.; Liao, G.; Guo, Z. Synthesis and Evaluation of GM2-monophosphoryl lipid A conjugate as a fully synthetic self-adjuvant cancer vaccine. *Sci. Rep.* **2017**, *7*, 11403.
(46) Wang, Q.; Zhou, Z.; Tang, S.; Guo, Z. Carbohydrate-monophosphoryl lipid A conjugates are fully synthetic self-adjuvanting cancer vaccines eliciting robust immune responses in the mouse. *ACS Chem. Biol.* **2012**, *7*, 235−240.
(47) Farah, F. S. Natural antibodies specific to the 2,4-dinitrophenyl group. *Immunology* **1973**, *25*, 217−226.
(48) Shahriar, I.; Kamra, M.; Kanduluru, A. K.; Campbell, C. L.; Nguyen, T. H.; Srinivasarao, M.; Low, P. S. Targeted recruitment of immune effector cells for rapid eradication of influenza virus infections. *Proc. Natl. Acad. Sci. U.S.A.* **2024**, *121*, No. e2408469121.
(49) Bournazos, S.; Wang, T. T.; Dahan, R.; Maamary, J.; Ravetch, J. V. Signaling by antibodies: Recent progress. *Annu. Rev. Immunol.* **2017**, *35*, 285−311.
(50) Jakobsche, C. E.; Parker, C. G.; Tao, R. N.; Kolesnikova, M. D.; Douglass, E. F. J.; Spiegel, D. A. Exploring binding and effector functions of natural human antibodies using synthetic immunomodulators. *ACS Chem. Biol.* **2013**, *8*, 2404−2411.
(51) Hossain, M. K.; Vartak, A.; Sucheck, S. J.; Wall, K. A. Liposomal Fc domain conjugated to a cancer vaccine enhances both humoral and cellular immunity. *ACS Omega* **2019**, *4*, 5204−5208.
(52) Hossain, M. K.; Vartak, A.; Karmakar, P.; Sucheck, S. J.; Wall, K. A. Augmenting vaccine immunogenicity through the use of natural human anti-rhamnose antibodies. *ACS Chem. Biol.* **2018**, *13*, 2130−2142.
(53) Zhou, K.; Hong, H.; Lin, H.; Gong, L.; Li, D.; Shi, J.; Zhou, Z.; Xu, F.; Wu, Z. Chemical synthesis of antibody-hapten conjugates capable of recruiting the endogenous antibody to magnify the Fc effector immunity of antibody for cancer immunotherapy. *J. Med. Chem.* **2022**, *65*, 323−332.
(54) Schwander, S.; Opravil, M.; Lüthy, R.; Hanson, D. G.; Schindler, J.; Dawson, A.; Letwin, B.; Dietrich, M. Phase I/II vaccination study of recombinant peptide F46 corresponding to the HIV-1 transmembrane protein coupled with 2.4 dinitrophenyl (DNP) Ficoll. *Infection* **1994**, *22*, 86−91.
(55) Sato, T.; Bullock, T. N. J.; Eisenlohr, L. C.; Mastrangelo, M. J.; Berd, D. Dinitrophenyl-modified autologous melanoma vaccine induces a T cell response to hapten-modified, melanoma peptides. *Clin. Immunol. Immunother.* **1997**, *85*, 265−272.
(56) Lotem, M.; Machlenkin, A.; Hamburger, T.; Nissan, A.; Kadouri, L.; Frankenburg, S.; Gimmon, Z.; Elias, O.; David, I. B.; Kuznetz, A.; Shiloni, E.; Peretz, T. Autologous melanoma vaccine induces antitumor and self-reactive immune responses that affect patient survival and depend on MHC class II expression on vaccine cells. *Clin. Cancer Res.* **2009**, *15*, 4968−4977.
(57) Dubrovska, A.; Kim, C.; Elliott, J.; Shen, W.; Kuo, T. H.; Koo, D. I.; Li, C.; Tuntland, T.; Chang, J.; Groessl, T.; Wu, X.; Gorney, V.; Ramirez-Montagut, T.; Spiegel, D. A.; Cho, C. Y.; Schultz, P. G. A chemically induced vaccine strategy for prostate cancer. *ACS Chem. Biol.* **2011**, *6*, 1223−1231.
(58) Lotem, M.; Merims, S.; Frank, S.; Hamburger, T.; Nissan, A.; Kadouri, L.; Cohen, J.; Straussman, R.; Eisenberg, G.; Frankenburg, S.; Carmon, E.; Alaiyan, B.; Shneibaum, S.; Ozge Ayyildiz, Z.; Isbilen, M.; Mert Senses, K.; Ron, I.; Steinberg, H.; Smith, Y.; Shiloni, E.; Gure, A. O.; Peretz, T. Adjuvant autologous melanoma vaccine for macroscopic stage III disease: Survival, biomarkers, and improved response to CTLA-4 blockade. *J. Immunol. Res.* **2016**, *2016*, 8121985.
(59) Hong, H.; Zhou, Z.; Zhou, K.; Liu, S.; Guo, Z.; Wu, Z. Site-specific C-terminal dinitrophenylation to reconstitute the antibody Fc functions for nanobodies. *Chem. Sci.* **2019**, *10*, 9331−9338.
(60) Liu, J.; Hong, H.; Shi, J.; Xie, Y.; Lu, Z.; Liu, Z.; Zhou, Z.; Bian, Z.; Huang, Z.; Wu, Z. Dinitrophenol-mediated modulation of an anti-PD-L1 VHH for Fc-dependent effector functions and prolonged serum half-life. *Eur. J. Pharmaceut. Sci.* **2021**, *165*, No. e105941.
(61) Kapcan, E.; Rullo, A. F. A covalent opsonization approach to enhance synthetic immunity against viral escape variants. *Cell Rep. Phys. Sci.* **2023**, *4*, 101258.
(62) Berd, D. Portrait of an autologous cancer vaccine: Then and now. *Hum. Vaccines Immunother.* **2023**, *19*, 2172925.
(63) Xu, Z.; Moyle, P. M. Bioconjugation approaches to producing subunit vaccines composed of protein or peptide antigens and covalently attached Toll-like receptor ligands. *Bioconjugate Chem.* **2018**, *29*, 572−586.
(64) Qureshi, N.; Kutuzova, G.; Takayama, K.; Rice, P. A.; Golenbock, D. T. Structure of lipid A and cell activation. *J. Endotoxin Res.* **1999**, *5*, 147−150.
(65) Morrison, D. C.; Silverstein, R.; Luchi, M.; Shnyra, A. Structure-function relationships of bacterial endotoxins. Contribution to microbial sepsis. *Infect. Dis. Clin. N. Am.* **1999**, *13*, 313−340.
(66) Darveau, R. P. Lipid A diversity and the innate host response to bacterial infection. *Curr. Opin. Microbiol.* **1998**, *1*, 36−42.
(67) Rietschel, E. T.; Kirikae, T.; Schade, F. U.; Mamat, U.; Schmidt, G.; Loppnow, H.; Ulmer, A. J.; Zahringer, U.; Seydel, U.; Di Padova, F.; Schreier, M.; Brade, H. Bacterial endotoxin: Molecular relationships of structure to activity and function. *FASEB J.* **1994**, *8*, 217−225.
(68) Stöver, A. G.; Correia, J. D. S.; Evans, J. T.; Cluff, C. W.; Elliott, M. W.; Jeffery, E. W.; Johnson, D. A.; Lacy, M. J.; Baldridge, J. R.; Probst, P.; Ulevitch, R. J.; Persing, D. H.; Hershberg, R. M. Structure-activity relationship of synthetic toll-like receptor 4 agonists. *J. Biol. Chem.* **2004**, *279*, 4440−4449.
(69) Zhou, Z.; Mondal, M.; Liao, G.; Guo, Z. Synthesis and evaluation of monophosphoryl lipid A derivatives as fully synthetic self-adjuvanting glycoconjugate cancer vaccine carriers. *Org. Biomol. Chem.* **2014**, *12*, 3238−3245.
(70) Speiser, D. E.; Romero, P. Molecularly defined vaccines for cancer immunotherapy, and protective T cell immunity. *Semin. Immunol.* **2010**, *22*, 144−154.
(71) Babu, J. S.; Nair, S.; Kanda, P.; Rouse, B. T. Priming for virus-specific CD8+ but not CD4+ cytotoxic T lymphocytes with synthetic lipopeptide is influenced by acylation units and liposome encapsulation. *Vaccine* **1995**, *13*, 1669−1676.
(72) Gupta, R. K.; Varanelli, C. L.; Griffin, P.; Wallach, D. F.; Siber, G. R. Adjuvant properties of non-phospholipid liposomes (Novasomes) in experimental animals for human vaccine antigens. *Vaccine* **1996**, *14*, 219−225.
(73) Estevez, F.; Carr, A.; Solorzano, L.; Valiente, O.; Mesa, C.; Barroso, O.; Victoriano Sierra, G.; Fernandez, L. E. Enhancement of the immune response to poorly immunogenic gangliosides after incorporation into very small size proteoliposomes (VSSP). *Vaccine* **1999**, *18*, 190−197.
(74) Alving, C. A.; Rao, M. Lipid A and liposomes containing lipid A as antigens and adjuvants. *Vaccine* **2008**, *26*, 3036−3045.
(75) Schoenborn, J. R.; Wilson, C. B. Regulation of interferon-gamma during innate and adaptive immune responses. *Adv. Immunol.* **2007**, *96*, 41−101.
(76) Tau, G.; Rothman, P. Biologic functions of the IFN-gamma receptors. *Allergy* **1999**, *54*, 1233−1251.
(77) Schroder, K.; Hertzog, P. J.; Ravasi, T.; Hume, D. A. Interferon-gamma: An overview of signals, mechanisms and functions. *J. Leukoc. Biol.* **2004**, *75*, 163−189.
(78) Bhat, M. Y.; Solanki, H. S.; Advani, J.; Khan, A. A.; Keshava Prasad, T. S.; Gowda, H.; Thiyagarajan, S.; Chatterjee, A.

https://doi.org/10.1021/jacsau.5c00187
JACS Au 2025, 5, 2210−2222

Comprehensive network map of interferon gamma signaling. *J. Cell Commun. Signal.* **2018**, *12*, 745−751.
(79) Stanley, E. R.; Berg, K. L.; Einstein, D. B.; Lee, P. S.; Pixley, F. J.; Wang, Y.; Yeung, Y. G. Biology and action of colony-stimulating factor-1. *Mol. Reprod. Dev.* **1997**, *46*, 4−10.
(80) Fixe, P.; Praloran, V. Macrophage colony-stimulating-factor (M-CSF or CSF-1) and its receptor: Structure-function relationships. *Eur. Cytokine Netw.* **1997**, *8*, 125−136.
(81) Parronchi, P.; De Carli, M.; Manetti, R.; Simonelli, C.; Sampognaro, S.; Piccinni, M. P.; Macchia, D.; Maggi, E.; Del Prete, G.; Romagnani, S. IL-4 and IFN (alpha and gamma) exert opposite regulatory effects on the development of cytolytic potential by Th1 or Th2 human T cell clones. *J. Immunol.* **1992**, *149*, 2977−2983.
(82) Silva-Filho, J. L.; Caruso-Neves, C.; Pinheiro, A. A. S. IL-4: An important cytokine in determining the fate of T cells. *Biophys. Rev.* **2014**, *6*, 111−118.
(83) Zhu, J. T helper 2 (Th2) cell differentiation, type 2 innate lymphoid cell (ILC2) development and regulation of interleukin-4 (IL-4) and IL-13 production. *Cytokine* **2015**, *75*, 14−24.
(84) Harris, N.; Gause, W. C. To B or not to B: B cells and the Th2-type immune response to helminths. *Trends Immunol.* **2011**, *32*, 80−88.
(85) Takatsu, K. Interleukin-5. *Curr. Opin. Immunol.* **1992**, *4*, 299−306.
(86) Sideras, P.; Noma, T.; Honjo, T. Structure and function of interleukin 4 and 5. *Immunol. Rev.* **1988**, *102*, 189−212.
(87) Schmidt-Arras, D.; Rose-John, S. IL-6 pathway in the liver: From physiopathology to therapy. *J. Hepatol.* **2016**, *64*, 1403−1415.
(88) Hirano, T. IL-6 in inflammation, autoimmunity and cancer. *Int. Immunol.* **2021**, *33*, 127−148.
(89) Akhtar, M.; Guo, S.; Guo, Y. F.; Zahoor, A.; Shaukat, A.; Chen, Y.; Umar, T.; Deng, P. G.; Guo, M. Upregulated-gene expression of pro-inflammatory cytokines (TNF-α, IL-1β and IL-6) via TLRs following NF-κB and MAPKs in bovine mastitis. *Acta Trop.* **2020**, *207*, 105458.
(90) de Waal Malefyt, R.; Haanen, J.; Spits, H.; Roncarolo, M. G.; te Velde, A.; Figdor, C.; Johnson, K.; Kastelein, R.; Yssel, H.; de Vries, J. E. Interleukin 10 (IL-10) and viral IL-10 strongly reduce antigen-specific human T cell proliferation by diminishing the antigen-presenting capacity of monocytes via downregulation of class II major histocompatibility complex expression. *J. Exp. Med.* **1991**, *174*, 915−924.
(91) Moore, K. W.; de Waal Malefyt, R.; Coffman, R. L.; O'Garra, A. Interleukin-10 and the interleukin-10 receptor. *Annu. Rev. Immunol.* **2001**, *19*, 683−765.
(92) Ma, X.; D'Andrea, A.; Kubin, M.; Aste-Amezaga, M.; Sartori, A.; Monteiro, J.; Showe, L.; Wysocka, M.; Trinchieri, G. Production of interleukin-12. *Res. Immunol.* **1995**, *146*, 432−448.
(93) Ma, X.; Trinchieri, G. Regulation of interleukin-12 production in antigen-presenting cells. *Adv. Immunol.* **2001**, *79*, 55−92.
(94) Trinchieri, G. Interleukin-12 and the regulation of innate resistance and adaptive immunity. *Nat. Rev. Immunol.* **2003**, *3*, 133−146.
(95) Hsieh, C. S.; Macatonia, S. E.; Tripp, C. S.; Wolf, S. F.; O'Garra, A.; Murphy, K. M. Development of TH1 CD4+ T cells through IL-12 produced by Listeria-induced macrophages. *Science* **1993**, *260*, 547−549.
(96) Zwirner, N. W.; Ziblat, A. Regulation of NK cell activation and effector functions by the IL-12 family of cytokines: The case of IL-27. *Front. Immunol.* **2017**, *8*, 25.
(97) Malek, T. R. The biology of interleukin-2. *Annu. Rev. Immunol.* **2008**, *26*, 453−479.
(98) Boyman, O.; Sprent, J. The role of interleukin-2 during homeostasis and activation of the immune system. *Nat. Rev. Immunol.* **2012**, *12*, 180−190.
(99) Malek, T. R.; Castro, I. Interleukin-2 receptor signaling: at the interface between tolerance and immunity. *Immunity* **2010**, *33*, 153−165.
(100) Lan, R. Y.; Selmi, C.; Gershwin, M. E. The regulatory, inflammatory, and T cell programming roles of interleukin-2 (IL-2). *J. Autoimmun.* **2008**, *31*, 7−12.
(101) Tian, H.; Xing, J.; Tang, X.; Sheng, X.; Chi, H.; Zhan, W. Interactions of interleukin 2 (IL-2) and IL-2 receptors mediate the activities of B lymphocytes in flounder (Paralichthys olivaceus). *Int. J. Biol. Macromol.* **2023**, *227*, 113−123.
(102) Gearing, A.; Thorpe, R.; Bird, C.; Spitz, M. Human B cell proliferation is stimulated by interleukin 2. *Immunol. Lett.* **1985**, *9*, 105−108.
(103) Kishi, H.; Inui, S.; Muraguchi, A.; Hirano, T.; Yamamura, Y.; Kishimoto, T. Induction of IgG secretion in a human B cell clone with recombinant IL 2. *J. Immunol.* **1985**, *134*, 3104−3107.
(104) Ciccia, F.; Guggino, G.; Ferrante, A.; Cipriani, P.; Giacomelli, R.; Triolo, G. Interleukin-9 and T helper type 9 cells in rheumatic diseases. *Clin. Exp. Immunol.* **2016**, *185*, 125−132.
(105) Fawaz, L. M.; Sharif-Askari, E.; Hajoui, O.; Soussi-Gounni, A.; Hamid, Q.; Mazer, B. D. Expression of IL-9 receptor alpha chain on human germinal center B cells modulates IgE secretion. *J. Allergy Clin. Immunol.* **2007**, *120*, 1208−1215.
(106) Rojas-Zuleta, W. G.; Sanchez, E. IL-9: Function, sources, and detection. *Methods Mol. Biol.* **2017**, *1585*, 21−35.
(107) Mills, K. H. G. IL-17 and IL-17-producing cells in protection versus pathology. *Nat. Rev. Immunol.* **2023**, *23*, 38−54.
(108) Sun, L.; Wang, L.; Moore, B. B.; Zhang, S.; Xiao, P.; Decker, A. M.; Wang, H. L. IL-17: Balancing protective immunity and pathogenesis. *J. Immunol. Res.* **2023**, *2023*, 3360310.
(109) Deshmane, S. L.; Kremlev, S.; Amini, S.; Sawaya, B. E. Monocyte chemoattractant protein-1 (MCP-1): An overview. *J. Interferon Cytokine Res.* **2009**, *29*, 313−326.
(110) Liu, Y.; Xu, K.; Xiang, Y.; Ma, B.; Li, H.; Li, Y.; Shi, Y.; Li, S.; Bai, Y. Role of MCP-1 as an inflammatory biomarker in nephropathy. *Front. Immunol.* **2024**, *14*, 1303076.
(111) Ushach, I.; Zlotnik, A. Biological role of granulocyte macrophage colony-stimulating factor (GM-CSF) and macrophage colony-stimulating factor (M-CSF) on cells of the myeloid lineage. *J. Leukoc. Biol.* **2016**, *100*, 481−489.
(112) Francisco-Cruz, A.; Aguilar-Santelises, M.; Ramos-Espinosa, O.; Mata-Espinosa, D.; Marquina-Castillo, B.; Barrios-Payan, J.; Hernandez-Pando, R. Granulocyte-macrophage colony-stimulating factor: not just another haematopoietic growth factor. *Med. Oncol.* **2014**, *31*, 774.
(113) Lopez-Castejon, G.; Brough, D. Understanding the mechanism of IL-1β secretion. *Cytokine Growth Factor Rev.* **2011**, *22*, 189−195.
(114) Varricchi, G.; Poto, R.; Marone, G.; Schroeder, J. T. IL-3 in the development and function of basophils. *Semin. Immunol.* **2021**, *54*, 101510.
(115) Dentelli, P.; Rosso, A.; Olgasi, C.; Camussi, G.; Brizzi, M. F. IL-3 is a novel target to interfere with tumor vasculature. *Oncogene* **2011**, *30*, 4930−4940.
(116) Payne, A. S.; Cornelius, L. A. The role of chemokines in melanoma tumor growth and metastasis. *J. Invest. Dermatol.* **2002**, *118*, 915−922.
(117) Appay, V.; Rowland-Jones, S. L. RANTES: A versatile and controversial chemokine. *Trends Immunol.* **2001**, *22*, 83−87.
(118) Berois, N.; Pittini, A.; Osinaga, E. Targeting Tumor Glycans for Cancer Therapy: Successes, Limitations, and Perspectives. *Cancers* **2022**, *14*, 645.
(119) Hu, H. G.; Li, Y. M. Emerging adjuvants for cancer immunotherapy. *Front. Chem.* **2020**, *8*, 601.
(120) Cuzzubbo, S.; Mangsbo, S.; Nagarajan, D.; Habra, K.; Pockley, A. G.; McArdle, S. E. B. Cancer vaccines: Adjuvant potency, importance of age, lifestyle, and treatments. *Front. Immunol.* **2021**, *11*, 615240.
(121) Pacheco, R.; Contreras, F.; Prado, C. Cells, molecules and mechanisms involved in the neuro-immune interaction. In *Cell Interaction*; Gowder, S., Ed.; IntechOpen: London, UK, 2012; pp 139−166.

https://doi.org/10.1021/jacsau.5c00187
JACS Au 2025, 5, 2210−2222